Available online at www.sciencedirect.com

ScienceDirect

journal homepage: www.elsevier.com/locate/he

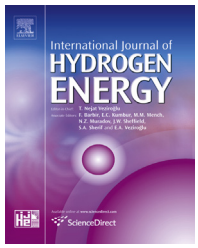

Direct steam reforming of diesel and diesel–biodiesel blends for distributed hydrogen generation

Stefan Martin [a,*], *Gerard Kraaij* [a], *Torsten Ascher* [a], *Penelope Baltzopoulou* [b], *George Karagiannakis* [b], *David Wails* [c], *Antje Wörner* [a]

[a] *German Aerospace Center (DLR), Institute of Technical Thermodynamics, Pfaffenwaldring 38–40, 70569 Stuttgart, Germany*

[b] *Aerosol & Particle Technology Lab., Chemical Process & Energy Resources Inst., Centre for Research & Technology Hellas (APTL/CPERI/CERTH), 6th km Charilaou-Thermi, P.O. Box: 60361, Thermi-Thessaloniki 57001, Greece*

[c] *Johnson Matthey Technology Centre, Blount's Court Sonning Common, Reading RG4 9NH, United Kingdom*

ARTICLE INFO

Article history:
Received 1 September 2014
Received in revised form
6 October 2014
Accepted 14 October 2014
Available online 6 November 2014

Keywords:
Hydrogen
Steam reforming
Diesel
Biodiesel
Liquid fuels

ABSTRACT

Distributed hydrogen generation from liquid fuels has attracted increasing attention in the past years. Petroleum-derived fuels with already existing infrastructure benefit from high volumetric and gravimetric energy densities, making them an interesting option for cost competitive decentralized hydrogen production.

In the present study, direct steam reforming of diesel and diesel blends (7 vol.% biodiesel) is investigated at various operating conditions using a proprietary precious metal catalyst. The experimental results show a detrimental effect of low catalyst inlet temperatures and high feed mass flow rates on catalyst activity. Moreover, tests with a desulfurized diesel–biodiesel blend indicate improved long-term performance of the precious metal catalyst. By using deeply desulfurized diesel (1.6 ppmw sulfur), applying a high catalyst inlet temperature (>800 °C), a high steam-to-carbon ratio (S/C = 5) and a low feed mass flow per open area of catalyst (11 g/h cm^2), a stable product gas composition close to chemical equilibrium was achieved over 100 h on stream. Catalyst deactivation was not observed.

Introduction

The lack of an existing hydrogen production and distribution infrastructure is widely considered an obstacle to an increased deployment of stationary and mobile fuel cell systems in the market [1–3]. In the transition phase towards sustainable hydrogen production (for instance by making use of excess wind energy and subsequent water electrolysis), it can be reasonable to produce hydrogen from liquid fuels with readily available infrastructure. Furthermore, liquid fuels offer the advantage of high gravimetric and volumetric energy densities.

* *Corresponding author*. Tel.: +49 711 6862 682; fax: +49 711 6862 665.
E-mail address: stefan.martin@dlr.de (S. Martin).

http://dx.doi.org/10.1016/j.ijhydene.2014.10.062

Today, the prevalent hydrogen production technology is steam reforming of natural gas [4]. However, centralized production suffers from additional hydrogen distribution costs. In contrast, on-board hydrogen production from liquid fuels for auxiliary power units (APUs) in heavy duty vehicles, which generally is regarded as an important early market for fuel cells in the transport sector [2], avoids the additional distribution-related costs, but suffers from a high level of system complexity. Therefore, several authors consider distributed hydrogen generation (DHG) from liquid fuels (diesel, biodiesel, methanol, ethanol etc.) to be a promising mid-term option for hydrogen production [3,5–9]. Hulteberg et al. [5] hypothesize that DHG systems will provide hydrogen at the lowest cost by 2020. DHG is currently being investigated in the framework of the FP7 project NEMESIS2+. Within this project a novel hydrogen generator (50 Nm^3/h) based on diesel and biodiesel is being developed for the purpose of integrating it into an existing refueling station. Apart from integrating such a system into refueling stations, on-site hydrogen generation from diesel is potentially applicable to the chemical industry, in particular for blanketing, hydrogenation and chemical synthesis.

Conversion of hydrocarbons into a hydrogen rich gas can be achieved via partial oxidation (POX), autothermal reforming (ATR) or steam reforming (SR). Among these three options, SR is currently the most established hydrogen production technology [10]. The product gas of SR is characterized by a high partial pressure of hydrogen (70–80 vol.% on a dry basis) compared to 40–50 vol.% for ATR and POX [11]. Drawbacks of the SR technology are a poor dynamic behavior and a comparatively high level of system complexity. Taking this into account, SR is widely considered as the preferred hydrogen production method for stationary applications [4,12].

While successful pre-reforming of diesel in the low temperature range (400–500 °C) using Ni-based catalysts has been demonstrated by several working groups [13,3,14], direct SR of diesel at high temperatures (~800 °C) is still at a relatively early research and development stage and needs further improvement [8]. Typically, diesel SR catalysts become deactivated within a few hours of on-stream exposure [15], which is mainly attributed to coking, sulfur poisoning and sintering of the catalyst [16].

Ming et al. carried out SR of diesel surrogate hexadecane using a proprietary catalyst formulation in a packed-bed reactor. Stable catalyst performance was shown for 73 h on stream without observing deactivation or carbon deposition [17]. Goud et al. conducted SR of hexadecane using a Pd/ZrO_2 catalyst coated on metal foils at steam-to-carbon ratios (S/C) of 3–6 and $T = 750$ °C–850 °C. A first-order kinetic model with a first-order deactivation rate was obtained. The catalyst deactivation rate was found to be accelerated by the presence of sulfur, at low S/C and at low temperatures [18].

In recent years, research groups have propagated the use of microstructured reactors for SR of diesel-like fuels, thereby circumventing problems related to heat and mass transfer limitations. Thormann et al. investigated hexadecane SR over a Rh/CeO_2 catalyst using microstructured devices [19,20]. The experiments revealed a fast transient response, thereby making it an interesting option for mobile APU applications. However, the reformer system suffered from high heat losses. Kolb et al. [21] developed a microstructured plate heat exchanger composed of stainless steel metal foils. Oxidative diesel steam reforming (molar O/C-ratio: 0.12–0.2) was performed using Euro V diesel supplied by Shell and using commercial catalysts provided by Johnson Matthey. Although a diesel conversion of 99.9% was achieved, formation of light hydrocarbons started after only a few hours of operation at $S/C < 4$ indicating the onset of catalyst deactivation. In a follow-up study, Grote et al. [22] carried out further steam reforming tests (4–10 kW thermal input) using a diesel surrogate mixture, accompanied by computational fluid dynamics modeling. The results show an increase of residual hydrocarbons (caused by deactivation of catalyst activity) with decreasing temperature. In order to prevent the formation of higher hydrocarbons, a reformer outlet temperature in excess of 1013 K was required. Long-term performance data was not presented by the authors. In a second follow-up study, Maximini et al. [23] tested four downscaled microchannel diesel steam reformers (1 kW_{th}) with different precious metal coatings at S/C ratios of 3 and 4. Increased carbon formation was observed when reducing the temperature from 800 °C to 700 °C. This was accompanied by the formation of higher hydrocarbons like C_2H_4, C_2H_2 and C_3H_6. The same group of authors presented experimental results of a microstructured diesel SR fuel processor coupled with a PEM fuel cell [24]. The 10 kW_{th} reformer consisted of 35 reformer channels with a channel height of 0.6 mm and 34 combustion channels being operated at $S/C = 5$ and 6 and a reactor outlet temperature of 765–800 °C. The results indicated a clear trend toward increasing residual hydrocarbon formation for higher feed mass flow rates. Furthermore, the stack voltage was observed to be highly sensitive to the residual hydrocarbon concentration in the reformate gas.

Other research groups used Ni-based catalysts for SR of diesel as Nickel is less expensive and more readily available than precious metals [6,15,25–27]. Fauteux-Lefebvre et al. [6] tested an Al_2O_3–ZrO_2-supported nickel–alumina spinel catalyst in a lab-scale isothermal packed-bed reactor at various operating conditions. Mixing of fuel and water was achieved by feeding in a stabilized hydrocarbon-water emulsion, which successfully prevented undesired pre-cracking. Product concentrations close to equilibrium for up to 20 h on-stream exposure were reported at severe operating conditions ($T < 720$ °C, $S/C < 2.5$). Steam reforming of commercial diesel was carried out for more than 15 h at $S/C < 2$. Carbon formation on the catalyst surface was not observed, although measured diesel conversion was lower than 90% [15].

Boon et al. were the first to report stable diesel steam reforming at temperatures of 800 °C using commercial precious metal catalysts [3]. The experiments were carried out in a packed-bed reactor at low gas hourly space velocities (GHSV) of 1000–2000 h^{-1}. Diesel evaporation was achieved by spraying diesel in a hot gas phase, thereby preventing self-pyrolysis during the evaporation step. Stable conditions with no sign of deactivation were reported for 143 h on stream at 1.2 bar, 800 °C and $S/C = 4.6$ and 2.6 using Aral Ultimate diesel with an added 6.5 ppm sulfur. Similar experiments with commercial BP Ultimate diesel containing 6 ppm sulfur turned out to be more challenging due to problems with blocking of

the diesel capillary and the nozzle. By using a medium sized diesel capillary (0.25 mm internal diameter) continuous operation was achieved for 180 h without observing any sign of deactivation, although deactivation occurred at larger diameters. The authors concluded that the observed deactivation was caused by the poor spraying of diesel, resulting in fluctuations of diesel conversion, thus initiating coke deposition.

The objective of this paper is to evaluate the applicability of direct steam reforming of diesel and diesel–biodiesel blends at various operating conditions using a proprietary precious metal based catalyst. The experimental study includes variation of reformer temperature, feed mass flow rate and diesel sulfur content. Special emphasis is placed on evaluating catalyst deactivation induced by coking and sulfur poisoning. Suitable operating conditions for stable steam reforming of diesel are determined, thus avoiding catalyst deactivation. The present study demonstrates the feasibility of direct high temperature steam reforming at elevated pressures, which advances the state of the art in this field.

Methodology

Diesel properties and chemical reaction system

Diesel is a complex mixture of paraffins, olefins, cycloalkanes and aromatics, containing up to 400 different hydrocarbon species, including organic sulfur compounds and additives [28]. Different empirical chemical formulae have been reported in the literature: $C_{12}H_{20}$ [15], $C_{14.342}H_{24.75}O_{0.0495}$ [29], $C_{13.4}H_{26.3}$ [30], $C_{13.57}H_{27.14}$ [31], $C_{16.2}H_{30.6}$ [32]. In the present study, a Shell diesel fulfilling EN 590 is used with the main properties given in Table 1. Based on the chemical analysis an empirical formula of $C_{13.3}H_{24.7}$ and a molecular weight of 185 g/mol was derived.

Steam reforming of diesel can be described by three independent equations, namely the conversion of hydrocarbons into carbon monoxide and hydrogen (Eq. (1)), the water–gas shift (WGS) reaction (Eq. (2)) and the methanation reaction (Eq. (3)). While the WGS and the methanation reactions are exothermic being favored at low temperatures, the diesel steam reforming reaction is endothermic, thus requiring external heat supply. Thermodynamics dictate that a high hydrogen yield is favored at high temperatures, high S/C and low pressures.

Table 1 – Diesel properties.

Property	Value	Test method
Density at $T = 15$ °C (kg/m^3)	836.4	ASTM D4052-11/ISO 12185-96
Lower heating value LHV (MJ/kg)	42.93	DIN 51,900-1,3
Monoaromatics (wt.%)	21.5	EN 12916
Polyaromatics (wt.%)	2.5	EN 12916
Total aromatic content (wt.%)	24.0	EN 12916
Sulfur content (ppmw)	7.0	ASTM D4294/EN 20884

$$C_nH_m + nH_2O \rightarrow nCO + (n + m/2)\,H_2 \quad \Delta H_{298\,K} \approx +150\ \text{kJ/mol} \tag{1}$$

$$CO + H_2O \leftrightarrow H_2 + CO_2 \quad \Delta H_{298\,K} = -41\ \text{kJ/mol} \tag{2}$$

$$CO + 3H_2 \leftrightarrow CH_4 + H_2O \quad \Delta H_{298\,K} = -206\ \text{kJ/mol} \tag{3}$$

The exact mechanism of diesel steam reforming is not completely understood. However, it is generally agreed that steam reforming of higher hydrocarbons takes place by irreversible adsorption on the catalyst surface resulting in C_1 compounds, followed by a surface reaction mechanism for conversion of C_1 species to yield gaseous CO [33,19]. CO is then converted to CO_2 through WGS reaction. The methanation reaction takes place simultaneously. Apart from the main SR reactions, undesired coking can occur (Eqs. (4–8)), leading to a gradual blocking of the active sites and subsequent catalyst deactivation. Elemental carbon can be formed directly from higher hydrocarbons (Eq. (4)), carbon monoxide (Eqs. (5) and (6)) and methane (Eq. (7)), or via polymerization of olefins/aromatics and subsequent stepwise dehydrogenation (Eq. (8)) [33]. The extent of the coking reactions strongly depends on reformer operating conditions such as temperature, steam-to-carbon ratio, gas hourly space velocity and reaction kinetics [34].

$$C_nH_m \rightarrow C + H_2 + CH_4 + \ldots \quad \Delta H_{298\,K} \geq 0\ \text{kJ/mol} \tag{4}$$

$$2CO \leftrightarrow C + CO_2 \quad \Delta H_{298\,K} = -172\ \text{kJ/mol} \tag{5}$$

$$CO + H_2 \leftrightarrow C + H_2O \quad \Delta H_{298\,K} = -131\ \text{kJ/mol} \tag{6}$$

$$CH_4 \leftrightarrow C + 2H_2 \quad \Delta H_{298\,K} = +75\ \text{kJ/mol} \tag{7}$$

$$\text{Olefines, Aromatics} \rightarrow \text{Polymers} \rightarrow \text{Coke} \quad \Delta H_{298\,K} \geq 0\ \text{kJ/mol} \tag{8}$$

It is well known that the catalysts used for diesel reforming are prone to deactivation by sulfur poisoning [35]. The main sulfur compounds in logistic fuels are mercaptanes, sulphides, disulphides, thiophenes, benzothiophenes (BT) and dibenzothiophenes (DBT). The prevailing sulfur species in commercial diesel are BTs and DBTs. Although the mechanism of sulfur poisoning of metallic catalysts is not fully understood, it is assumed that metal poisoning by sulfur compounds involves strong chemisorption of the sulfur-containing molecule on the metal sites (Eq. (9)), leading to a stable and inactive metal sulfide species on the catalyst surface (Eq. (10)) [33]. In contrast to catalyst coking, sulfur poisoning is very difficult to reverse, requiring harsh conditions for catalyst regeneration [15].

$$M + S - R \rightarrow M + R' + H_2S \tag{9}$$

$$H_2S + M \rightarrow M - S + H_2 \tag{10}$$

Experimental test set-up

The flow sheet and the main components of the test-rig employed in the present study are shown in Fig. 1. Water and diesel are fed into the reformer using mass flow controllers and micro annular gear pumps. Diesel at $T = 0\,^{\circ}C$ is mixed with superheated steam ($T = 390\,^{\circ}C$) before being heated by an electrical oven to the desired SR temperature. The catalytic conversion into H_2, CO, CO_2 and CH_4 is accomplished by using a metal-based catalyst monolith which is mounted inside a stainless steel tube (d = 2.1 cm). The catalyst monolith (600 cpsi, l = 5.1 cm, d = 2.03 cm) is coated with finely distributed platinum group metals. The catalyst comprised Rh on a high surface area (140 m^2/g), alumina based mixed metal oxide support. It was coated onto the monolith at a loading of 0.122 g catalyst/cm^3 with an overall Rh loading of 2440 g/m^3. The reformer temperature is controlled via the catalyst outlet temperature TD.

Nickel alloy thermocouples (type k) have been used in this study with a specified measurement error of ±2.5 K. By placing four thermocouples along the axis of the catalyst piece (TA, TB, TC, TD, see Fig. 1), the temperature profile can be measured over time on stream. The axial temperature profile provides valuable information on catalyst activity. After initiation of the reforming reaction, the temperature at the catalyst inlet drops due to the endothermic heat demand of the SR reaction. A stable catalyst inlet temperature over time indicates stable catalyst activity, whereas a temperature increase is accompanied by a loss of catalyst activity.

Upon leaving the reformer section, water and unconverted diesel are condensed in a cold trap at $T = 10\,^{\circ}C$ and stored in a condensate reservoir. Before each experiment, the cold trap is filled with 100 ml of organic solvent (dodecane, mixture of isomers). The fuel conversion rate FCR, (Eq. (11)) is subsequently derived from gas chromatography (GC) analysis of the organic phase that accumulates in the cold trap during the test. GC analysis of the condensate was found to be more reliable than determining the fuel conversion via the gas phase. In addition, carbon deposition on the catalyst surface and the tube walls and higher hydrocarbons leaving the cold trap are considered for FCR calculations:

$$\mathrm{FCR} = \frac{m_D - (m_{D,liq.} + m_C + m_{HCs})}{m_D} \tag{11}$$

The amount of condensed diesel and its cracking products in the cold trap $m_{D,liq.}$ is derived from the area proportion $x_{D,liq.}$ in the gas chromatogram (which is assumed to be equivalent to the mass proportion) and the amount of dodecane m_{Dod} according to Eq. (12). The amount of deposited carbon m_C is obtained by flushing the system with air after each test and detecting the resulting CO_2 evolution. Higher hydrocarbons m_{HCs} (C_2–C_4) passing the cold trap are measured periodically via GC analysis (Varian Micro CP-4900, accuracy: ±0.1% of the upper limit range).

$$m_{D,liq.} = m_{Dod} \cdot \left(\frac{1}{1 - x_{D,liq.}} - 1 \right) \tag{12}$$

Downstream of the cold trap, any remaining moisture is removed by an aerosol filter. The dry reformate gas flow is measured with a mass flow controller before it enters the online gas analyzer unit (Rosemount Analytical NGA 2000 MLT), which is equipped with an infrared adsorption detector for CO, CO_2 and CH_4 and a thermal conductivity detector for measurement of H_2. The specified measurement error is ±1% relative to the full scale value.

Accordingly, the mass balance of the process is given by:

$$m_{diesel} + m_{water} = m_{condensate} + m_{moisture,residual} + m_{reformate,dry}$$

A mass balance error (defined as $|1 - m_{product}/m_{feed}|$) of <2% was determined for all SR experiments presented in this study.

Parameters

The gas hourly space velocity GHSV at standard temperature and pressure (STP) and the molar steam-to-carbon ratio S/C are defined as follows:

$$\mathrm{GHSV} = \frac{\dot{V}_{Feed,STP}}{V_{cat.}} \tag{13}$$

$$S/C = \frac{\dot{n}_{H_2O}}{\dot{n}_{Diesel,C}} \tag{14}$$

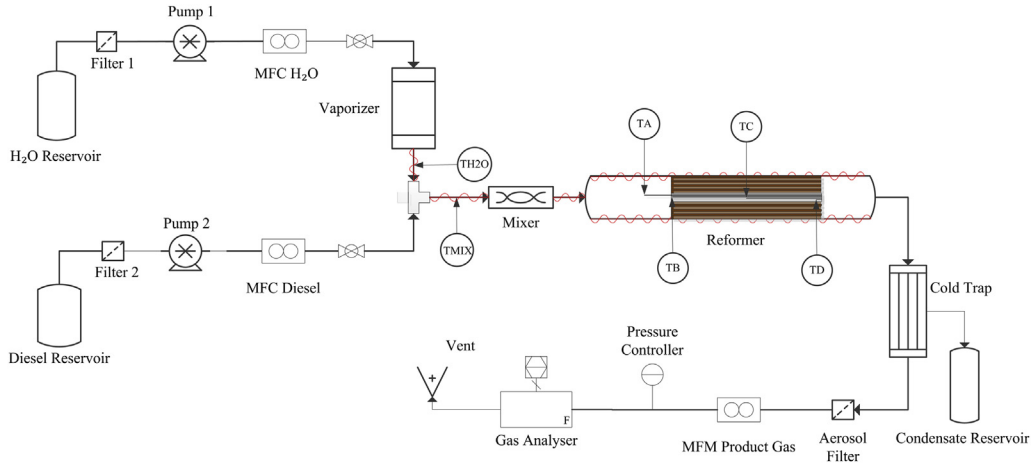

Fig. 1 – Schematic of diesel steam reforming test rig.

Results and discussion

Steam reforming of pure diesel

Steam reforming at $T = 800\ ^{\circ}C$, $p = 3$ bar and $S/C = 5$ has been carried out using pure diesel ($m_{Diesel} = 5$ g/h) the properties of which are described in Table 1. As can be seen from Fig. 2 a stable product gas composition close to chemical equilibrium has been achieved over 20 h on stream. No higher hydrocarbons have been detected in the product gas stream, while methane production was also negligible.

It is well known that it is not possible to quantify the onset of catalyst deactivation by analyzing the product gas alone [3], which is due to the fact that parts of the catalyst can already be heavily deactivated before a deterioration of the product gas composition (decrease of H_2, increase of CH_4, formation of higher hydrocarbons) can be observed. A more precise method of determining the onset of catalyst deactivation is to measure the temperature at the center line of the catalyst. Fig. 3 depicts the axial catalyst temperatures over time on stream. Shortly after initiation of the reforming reaction, the catalyst entrance temperature TB drops by 27 °C due to the endothermic nature of the process. Subsequently, it stabilizes at this level indicating a stable catalyst activity.

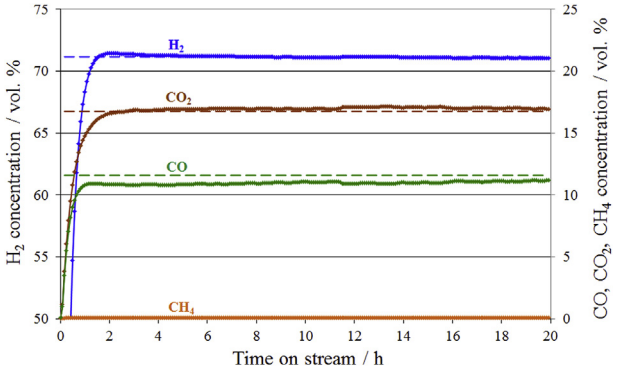

Fig. 2 – Dry product gas composition of diesel steam reforming ($T = 800\ ^{\circ}C$, $p = 3$ bar and $S/C = 5$).

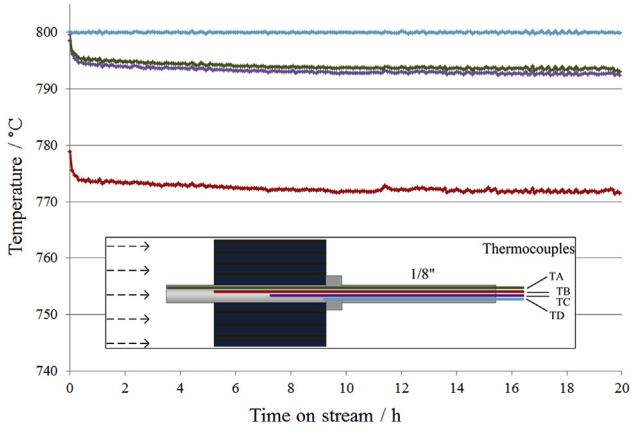

Fig. 3 – Axial catalyst temperatures over time on stream ($T = 800\ ^{\circ}C$, $p = 3$ bar and $S/C = 5$).

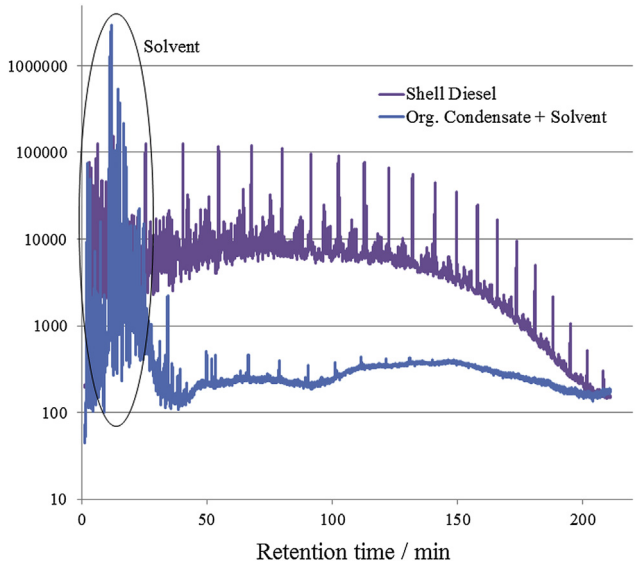

Fig. 4 – Gas chromatography analysis ($T = 800\ ^{\circ}C$, $p = 3$ bar and $S/C = 5$).

As can be seen from the GC analysis (Fig. 4) the diesel compounds (predominantly paraffins) are for the most part converted into gaseous products during the steam reforming step. Only small amounts of unconverted hydrocarbon species remain in the liquid organic condensate. Based on Eq. (11), a fuel conversion rate of 97.6% was calculated. 85% of the unconverted diesel is attributed to coke deposition on the catalyst surface and on the tube walls (m_C), whilst the

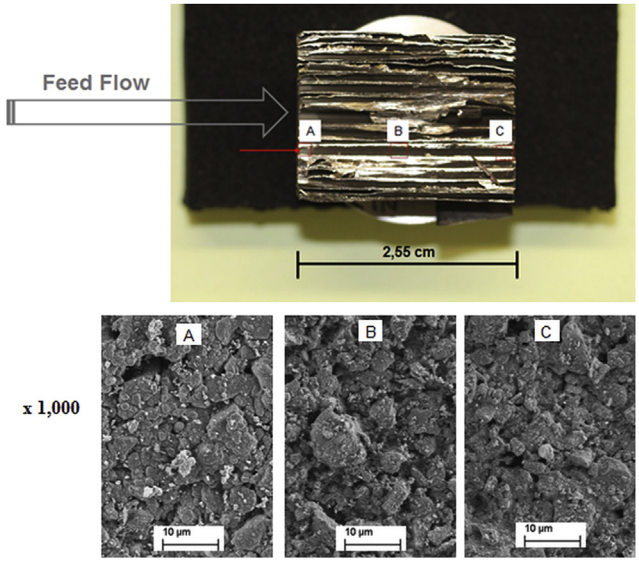

Fig. 5 – Cross section of spent metallic catalyst monolith (top), scanning electron microscopy of the catalyst surface at different positions (bottom).

Table 2 – Comparison of shell diesel and B7 diesel properties.

Property	Diesel	B7 Diesel/desulfurized B7 Diesel
Density at $T = 15\ ^\circ C$ (kg/m^3)	836.4	831.5/828.4
Lower heating value LHV (MJ/kg)	42.93	42.63/43.11
Empirical formula	$C_{13.3}H_{24.7}$	$C_{13.5}H_{25.2}O_{0.1}$
Sulfur content (ppmw)	7.0	6.8/1.6
Fatty acid methyl ester FAME (vol.%)	<0.3	7/7
Total aromatic content (wt. %)	24.0	18.7/15.3

remaining 15% are attributed to unconverted diesel compounds and its cracking products ($m_{D,liq.}$).

In addition, the spent catalyst has been analyzed by scanning electron microscopy (SEM), revealing slight sintering at the catalyst inlet (Fig. 5), which is accompanied by a reduction of surface porosity. In our previous study with feedstock biodiesel, similar sintering effects were observed [36]. However, sintering was more severe, especially when using ceramic based catalyst monoliths, leading to a reduction of catalytically active sites for biodiesel conversion. In the case of diesel SR with metallic monoliths, the observed sintering is not detrimental to catalyst stability in the given time on-stream.

Steam reforming of diesel blends

In addition to the experiment with pure diesel, steam reforming tests with diesel containing 7 vol.% biodiesel (B7 diesel) were carried out. The B7 diesel was acquired from a local petrol station. The physical properties of the B7 diesel differ slightly from the Shell diesel (Table 2). 5 g/h of B7 diesel were fed into the reformer at $S/C = 5$ and $p = 5$ bar.

As can be seen from Fig. 6, a stable product gas composition has been achieved over 100 h on stream. H_2, CO_2 and CH_4 concentrations are in equilibrium, whereas CO shows slight deviations. As expected, CH_4 is not present in the product gas stream at the given catalyst outlet temperature of 850 °C, which is attributed to the exothermic nature of the methanation reaction (see Eq. (3)). Equilibrium gas concentrations (dashed lines) based on reformer outlet temperature TD were calculated using Aspen Plus® applying minimization of free Gibbs energy. For more details of this widely used method please refer to Lin et al. [37]. Higher hydrocarbons were not detected in the dry product gas stream after leaving the cold trap, nor are they expected from equilibrium calculations.

After initiation of the reforming reaction, the catalyst inlet temperature TB drops by 52 °C, subsequently stabilizing at this level (Fig. 7). However, after 68 h on stream, temperature TB starts to rise, indicating the onset of catalyst deactivation. Compared to the test with pure diesel (Fig. 3), the temperature drop at the catalyst front end is larger, which might be attributed to the higher catalyst loading (0.183 g/cm^3 for B7 diesel versus 0.122 g/cm^3 for pure diesel).

In a test at similar operating conditions ($T = 850\ ^\circ C$, $p = 5$ bar, $S/C = 5$) with desulfurized B7 diesel (produced by liquid-phase adsorption of organic diesel compounds using a specific activated carbon-based sorbent [38]) a stable product gas composition was achieved over 100 h (not shown here since the measured product concentration profiles were very similar to the ones depicted in Fig. 6), with no higher hydrocarbons being present in the dry reformate stream. The fuel conversion rate, as defined by Eq. (11), was slightly higher than that of the sulfur-containing B7 diesel (98.7% versus 98.5%). Moreover, the catalyst inlet temperature TB, which is an appropriate indicator for catalyst activity, was found to be more stable (Fig. 8 vs. Fig. 7). Nevertheless, a minor increase in TB was observed after 96 h. It is uncertain if this slight temperature increase is a sign of catalyst deactivation, considering that the deviation is still within the statistical range of fluctuations. It can therefore be hypothesized that the reformer catalyst activity is higher for the desulfurized diesel, indicating an appreciable effect of organic sulfur compounds

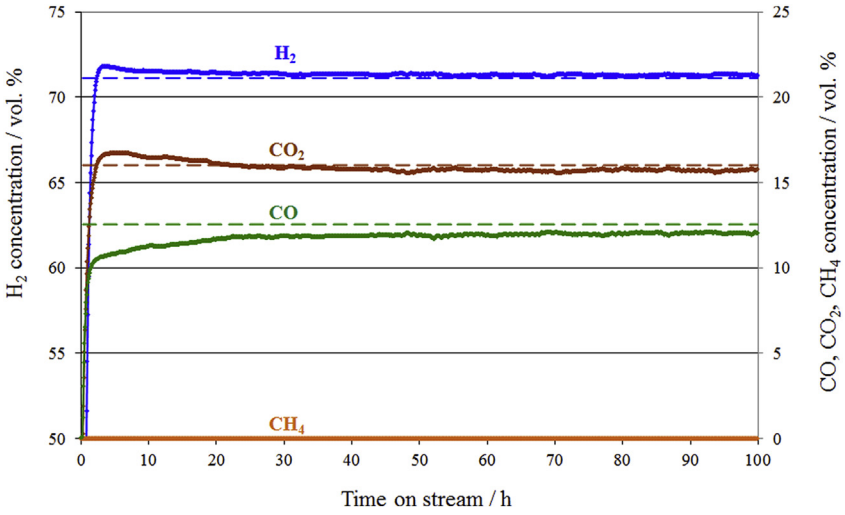

Fig. 6 – Dry product gas composition (B7 diesel, 6.8 ppm sulfur, $T = 850\ ^\circ C$, $p = 5$ bar and $S/C = 5$).

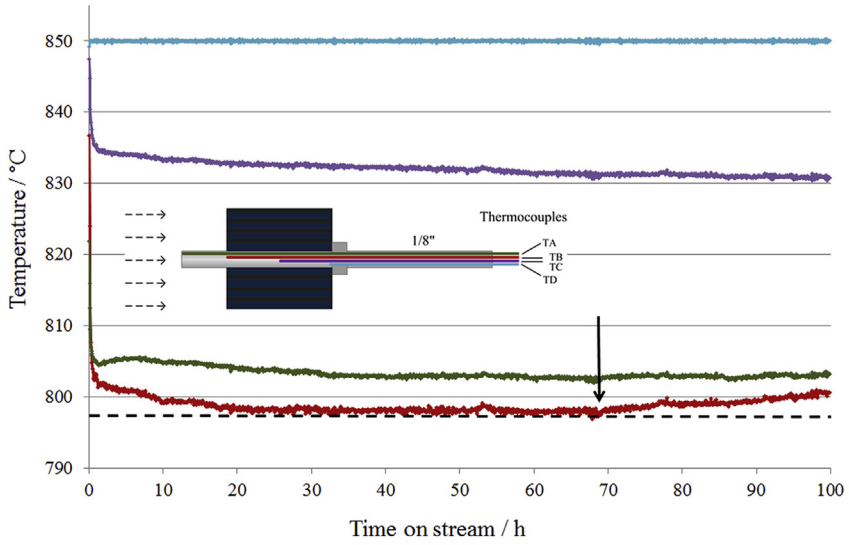

Fig. 7 – Axial catalyst temperatures (B7 diesel, 6.8 ppm sulfur, $T = 850$ °C, $p = 5$ bar, $S/C = 5$).

on long-term reformer performance. This ties in well with the requirement to desulfurize petroleum-derived liquid fuels to sulfur levels of less than 1 ppmw in order to be used in fuel cell systems [39].

Compared to the test with pure diesel (see Figs. 2–5) the conversion rates for the B7 type diesel batches (original and desulfurized) are about one percentage point higher. This might be attributed to the higher reforming temperature (850 °C vs. 800 °C) and to the fact that biodiesel, being present with a share of 7 vol.% in B7 diesel, can be more easily converted into gaseous products, as it is free of aromatic compounds. It is well known that aromatics are amongst the least reactive components in liquid fuels, thus requiring higher temperatures than non-aromatic compounds in order to be fully converted [40,41]. In addition, aromatic compounds are one of the main coke precursors, leading to coke deposition and subsequent catalyst deactivation [42].

Feed mass flow variation

Recently, several authors have presented results of liquid fuel reforming, indicating a detrimental effect of high feed mass flow rates on catalyst activity. For ATR of diesel, Lin et al. [43] reported initiation of carbon formation at GHSV > 48,500 h^{-1} (compared to > 44,000 for biodiesel), being accompanied by an increase of light hydrocarbons. Ethylene, aromatics and naphtenes were identified as the main precursors for carbon formation [37]. Concurrently, Engelhardt et al. [24] observed a clear trend toward a higher amount of hydrocarbons for increasing diesel feed flow. For SR of biodiesel, Martin at al. [36] reported initiation of catalyst deactivation at GHSV levels in excess of 4400 h^{-1} (corresponding to a mass flow per open area of catalyst of 21 g/h cm^2 and a fluid velocity of 5 cm/s) at a catalyst inlet temperature of 730 °C.

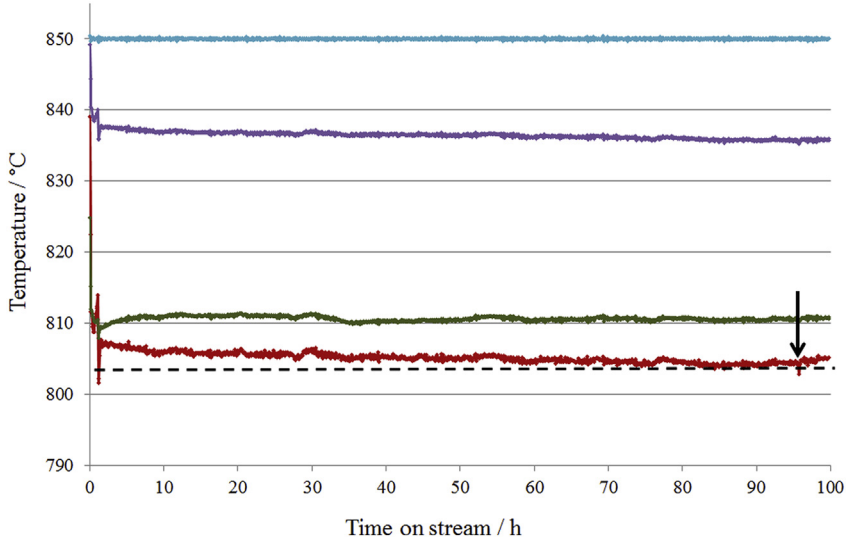

Fig. 8 – Axial catalyst temperatures (B7 diesel, 1.6 ppm sulfur, $T = 850$ °C, $p = 5$ bar, $S/C = 5$).

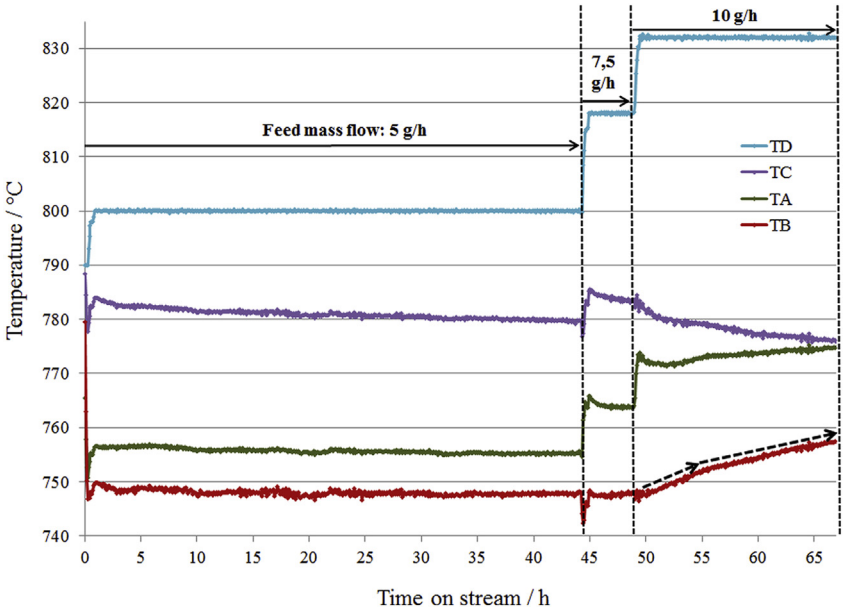

Fig. 9 – Feed mass flow variation (B7 diesel, 6.8 ppm sulfur, $T_{in} = 750$ °C, $p = 5$ bar, $S/C = 5$).

In the present study, the fuel mass flow has been increased stepwise from 5 g/h to 10 g/h at an initial catalyst inlet temperature of 750 °C in order to evaluate the influence of increasing feed mass flow rates on catalyst deactivation for SR of diesel blends. As can be seen from Fig. 9, the catalyst inlet temperature TB remains constant for diesel mass flows up to 7.5 g/h. Upon raising the mass flow to 10 g/h, the catalyst inlet temperature TB increases, indicating initiation of catalyst deactivation due to coking and/or sulfur poisoning. Thus, a threshold mass flow per open area of catalyst of 17 g/h cm^2 (corresponding to a fluid velocity of 4 cm/s and GHSV of 3700 h^{-1}) must not be exceeded in order to prevent initiation of catalyst deactivation. Obviously, the threshold value for the diesel blend considered in this study is lower than for biodiesel. Thus, high feed mass flows are a critical issue for diesel steam reforming.

Conclusions

Direct diesel steam reforming has been evaluated experimentally at various operating conditions using precious-metal-based catalyst monoliths. By cooling the feed diesel to 0 °C and mixing it directly into superheated steam ($T = 390$ °C) coke deposition in the mixing zone and on the catalyst surface could be reduced to a minimum and fluctuations of the product gas flow were avoided.

Successful direct steam reforming of pure diesel and diesel blends (B7) with stable product gas composition near chemical equilibrium has been achieved by applying a steam-to-carbon ratio of 5, a high catalyst inlet temperature (~800 °C) and a low gas hourly space velocity (2200–2500 h^{-1}). Diesel conversion ranged from 97.6% for pure diesel to 98.7% for desulfurized B7 diesel. In the case of pure diesel, scanning electron microscopy revealed slight sintering effects at the catalyst inlet, which however, were not detrimental for catalyst performance in the time range studied.

Catalyst durability tests (100 h) with diesel blends indicate a slightly higher catalyst activity for desulfurized B7 diesel (1.6 ppmw sulfur) compared to the original B7 diesel (6.8 ppmw sulfur). We therefore recommend to desulfurize commercial diesel blends to less than 2 ppmw prior to steam reforming, in order to maintain a high and stable catalyst activity. Thereby, operation and maintenance costs for distributed hydrogen generation systems can be reduced substantially.

Furthermore, the experimental results reveal a detrimental effect of high feed mass flow rates on catalyst activity. At given boundary conditions ($T_{in} = 750$ °C, $p = 5$ bar, $S/C = 5$) catalyst deactivation caused by coking and/or sulfur poisoning is initiated at a threshold mass flow per open area of catalyst of 17 g/h cm^2 (corresponding to a fluid velocity of 4 cm/s and gas hourly space velocity of 3700 h^{-1}). As a rule of thumb, the maximum threshold feed mass flow for steam reforming of diesel is less than half the threshold value of biodiesel, making biodiesel an interesting alternative feedstock for distributed hydrogen generation via SR.

Summarizing, successful direct steam reforming of diesel and diesel–biodiesel blends at elevated pressures (3–5 bar) has been shown on a lab-scale level. Applying a high catalyst inlet temperature (>750 °C) and low feed mass flow rates per open area of catalyst (≤17 g/h cm^2) proved decisive for stable long-term operation. Future work should be dedicated to carrying out reformer design studies, allowing for higher diesel throughputs, thus lowering the costs of distributed hydrogen production.

Acknowledgment

The authors gratefully acknowledge the support of the Fuel Cells and Hydrogen Joint Technology Initiative under Grant

Agreement No. 278138. The HIFUEL precious metal catalysts used in this study were kindly provided by Johnson Matthey. The desulfurized diesel was provided by the Aerosol and Particle Technology Laboratory of the Centre for Research and Technology Hellas (APTL/CERTH). The biodiesel was supplied by Abengoa Bioenergy. For proofreading the manuscript we thank Martin Kraenzel.

REFERENCES

[1] Pettersson LJ, Westerholm R. State of the art of multi-fuel reformers for fuel cell vehicles: problem identification and research needs. Int J Hydrogen Energy 2001;26:243–64.
[2] Contestabile M. Analysis of the market for diesel PEM fuel cell auxiliary power units onboard long-haul trucks and of its implications for the large-scale adoption of PEMFCs. Energy Policy 2010;38:5320–34.
[3] Boon J, van Dijk E, de Munck S, van den Brink R. Steam reforming of commercial ultra-low sulphur diesel. J Power Sources 2011;196:5928–35.
[4] Holladay JD, Hu J, King DL, Wang Y. An overview of hydrogen production technologies. Catal Today 2009;139:244–60.
[5] Hulteberg PC, Burford H, Duraiswamy K, Porter B, Woods R. A cost effective steam reformer for a distributed hydrogen infrastructure. Int J Hydrogen Energy 2008;33:1266–74.
[6] Fauteux-Lefebvre C, Abatzoglou N, Blanchard J, Gitzhofer F. Steam reforming of liquid hydrocarbons over a nickel-alumina spinel catalyst. J Power Sources 2010;195:3275–83.
[7] Levin DB, Chahine R. Challenges for renewable hydrogen production from biomass. Int J Hydrogen Energy 2010;35:4962–9.
[8] Specchia S. Fuel processing activities at European level: a panoramic overview. Int J Hydrogen Energy 2014;39:17953–68.
[9] Nahar G, Dupont V. Recent advances in hydrogen production via autothermal reforming process (ATR): a review of patents and research articles. Recent Pat Chem Eng 2013;6:8–42.
[10] Nahar G, Dupont V. Hydrogen via steam reforming of liquid biofeedstock. Biofuels 2012;3(2):167–91.
[11] Ersoz A, Olgun H, Ozdogan S. Reforming options for hydrogen production from fossil fuels for PEM fuel cells. J Power Sources 2006;154:67–73.
[12] Martin S, Wörner A. On-board reforming of biodiesel and bioethanol for high temperature PEM fuel cells: comparison of autothermal reforming and steam reforming. J Power Sources 2011;196(6):3163–71.
[13] Piwetz MM, Larsen JS, Christensen TS. Hydrodesulfurization and prereforming of logistic fuels for use in fuel cell applications, fuel cell seminar program and abstracts. 1996.
[14] Koo KY, Park MG, Jung UH, Kim SH, Yoon WL. Diesel pre-reforming over highly dispersed nano-sized Ni catalysts supported on MgO–Al_2O_3 mixed oxides. Int J Hydrogen Energy 2014;39:10941–50.
[15] Fauteux-Lefebvre C, Abatzoglou N, Braidy N, Achouri IE. Diesel steam reforming with a nickel-alumina spinel catalyst for solid oxide fuel cell application. J Power Sources 2011;196:7673–80.
[16] Bartholomew CH, Farrauto RJ. Fundamentals of industrial catalytic processes. 2nd ed. Wiley; 2006.
[17] Ming Q, Healey T, Allen L, Irving P. Steam reforming of hydrocarbon fuels. Catal Today 2002;77:51–64.
[18] Goud SK, Whittenberger WA, Chattopadhyay S, Abraham MA. Steam reforming of *n*-hexadecane using a Pd/ZrO_2 catalyst: kinetics of catalyst deactivation. Int J Hydrogen Energy 2007;32:2868–74.
[19] Thormann J, Maier L, Pfeifer P, Kunz U, Deutschmann O, Schubert K. Steam reforming of hexadecane over a Rh/CeO_2 catalyst in microchannels: experimental and numerical investigation. Int J Hydrogen Energy 2009;34:5108–20.
[20] Thormann J, Pfeifer P, Kunz U. Dynamic performance of hexadecane steam reforming in a microstructured reactor. Chem Eng J 2012;191:410–5.
[21] Kolb G, Hofmann C, O'Connell M, Schürer J. Microstructured reactors for diesel steam reforming, water–gas shift and preferential oxidation in the kiloWatt power range. Catal Today 2009;147S:S176–84.
[22] Grote M, Maximini M, Yang Z, Engelhardt P, Köhne H, Lucka K, et al. Experimental and computational investigations of a compact steam reformer for fuel oil and diesel fuel. J Power Sources 2011;196:9027–35.
[23] Maximini M, Engelhardt P, Grote M, Brenner M. Further development of a microchannel steam reformer for diesel fuel. Int J Hydrogen Energy 2012;37:10125–34.
[24] Engelhardt P, Maximini M, Beckmann F, Brenner M. Integrated fuel cell APU based on a compact steam reformer for diesel and a PEMFC. Int J Hydrogen Energy 2012;37:13470–7.
[25] Achouri IE, Abatzoglou N, Fauteux-Lefebvre C, Braidy N. Diesel steam reforming: comparison of two nickel aluminate catalysts prepared by wet-impregnation and co-precipitation. Catal Today 2013;207:13–20.
[26] Xu L, Mi W, Su Q. Hydrogen production through diesel steam reforming over rare-earth promoted Ni/γ-Al_2O_3 catalysts. J Nat Gas Chem 2011;20:287–93.
[27] Zyryanova MM, Badmaev SD, Belyaev VD, Amosov YI, Snytnikov PV, Kirillov VA, et al. Catalytic reforming of hydrocarbon feedstocks into fuel for power generation units. Catal Oil Ref 2013;5:312–7.
[28] Parmar RD, Kundu A, Karan K. Thermodynamic analysis of diesel reforming process: mapping of carbon formation boundary and representative independent reactions. J Power Sources 2009;194:1007–20.
[29] Sahin Z. Experimental and theoretical investigation of the effects of gasoline blends on single-cylinder diesel engine performance and exhaust emissions. Energy Fuel 2008;22:3201–12.
[30] Pereira C, Bae J-M, Ahmed S, Krumpelt M. Liquid fuel reformer development: autothermal reforming of diesel fuel. Argonne National Laboratory, Electrochemical Technology Program; 2000.
[31] Brown LF. A comparative study of fuels for on-board hydrogen production for fuel-cell-powered automobiles. Int J Hydrogen Energy 2001;26:381–97.
[32] Lindermeir A, Kah S, Kavurucu S, Mühlner M. On-board diesel fuel processing for an SOFC-APU – technical challenges for catalysis and reactor design. Appl Catal B Environ 2007;70:488–97.
[33] Navarro Yerga RM, Alvarez-Galvan MC, Mota N, Villoria de la Mano JA, Al-Zahrani SM, Fierro JLG. Catalysts for hydrogen production from heavy hydrocarbons. ChemCatChem 2011;3:440–57.
[34] Mieville RL. Coking characteristics of reforming catalysts. J Catal 1986;100:482–8.
[35] Hulteberg C. Sulphur-tolerant catalysts in small-scale hydrogen production, a review. Int J Hydrogen Energy 2012;37:3978–92.
[36] Martin S, Kraaij G, Ascher T, Wörner A, Wails D. An experimental investigation of biodiesel steam reforming. Int J Hydrogen Energy (accepted 30 October 2014).
[37] Lin J, Trabold TA, Walluk MR, Smith DF. Autothermal reforming of biodiesel–ethanol–diesel blends for solid oxide fuel cell applications. Energy Fuel 2013;27:4371–85.

[38] Hoguet JC, Karagiannakis GP, Valla JA, Agrafiotis CC, Konstandopoulos AG. Gas and liquid phase fuels desulphurization for hydrogen production via reforming processes. Int J Hydrogen Energy 2009;34:4953–62.
[39] van Rheinberg O, Lucka K, Köhne H. About the process improvement of adsorptive desulphurisation by adding hydrogen donators as additives in liquid fuels. J Power Sources 2011;196:8983–93.
[40] Wang X, Gorte RJ. A study of steam reforming of hydrocarbon fuels on Pd/ceria. Appl Catal A Gen 2002;224:209–18.
[41] Gonzalez AV, Pettersson LJ. Full-scale autothermal reforming for transport applications: the effect of diesel fuel quality. Catal Today 2013;210:19–25.
[42] Nahar GA. Hydrogen rich gas production by the autothermal reforming of biodiesel (FAME) for utilization in the solid-oxide fuel cells: a thermodynamic analysis. Int J Hydrogen Energy 2010;35:8891–911.
[43] Lin J, Trabold TA, Walluk MR, Smith DF. Bio-fuel reforming for solid oxide fuel cell applications. Part 2: biodiesel. Int J Hydrogen Energy 2014;39:183–95.